Construction and Building Materials 265 (2020) 120660

Contents lists available at ScienceDirect

Construction and Building Materials

journal homepage: www.elsevier.com/locate/conbuildmat

On the versatility of paper pulp as a viscosity modifying admixture for cement composites

H. Karimi [a], F. Gauvin [a], H.J.H. Brouwers [a], R. Cardinaels [b], Qingliang Yu [a,c,*]

[a] Department of the Built Environment, Eindhoven University of Technology, P.O. Box 513, 5600 MB Eindhoven, The Netherlands
[b] Department of Mechanical Engineering, Eindhoven University of Technology, P.O. Box 513, 5600 MB Eindhoven, The Netherlands
[c] School of Civil Engineering, Wuhan University, 430072 Wuhan, PR China

HIGHLIGHTS

- An innovative viscosity-modifying admixture (VMA) is produced from paper pulp.
- The versatility of using milled paper pulp as a VMA in cement composites is validated.
- The mechanism of viscosity modifying action of milled paper pulp is elaborated.
- A new parameter is proposed to quantify nonlinearity induced by VMAs.

ARTICLE INFO

Article history:
Received 17 March 2020
Received in revised form 30 July 2020
Accepted 17 August 2020
Available online 11 September 2020

Keywords:
Paper pulp
Cement grout
Viscosity-modifying admixture
Rheology
Compressive strength

ABSTRACT

In this paper, we report the performance of paper pulp as an innovative viscosity modifying admixture (VMA) for cement composites. Two different levels of fineness were obtained by mechanical milling of the same source of paper pulp. Their effects on viscosity modification, hydration kinetics, autogenous shrinkage, and compressive strength of cement grouts were measured, and their structural integrity at high pH was assessed. A new parameter was proposed to quantify nonlinearity induced by VMAs. Results showed that the hierarchical structure of paper pulp makes it possible to activate bridging flocculation and swelling mechanisms of hydrophile paper pulp fibers at different levels to produce versatile VMAs. The coarser milled paper pulp fibers mainly influences the plastic viscosity. By contrast, the milled paper pulp consisting of ultra-fine fibers significantly modifies both plastic viscosity and dynamic yield stress, induces more nonlinearity in the mixtures, and increases compressive strength of mortars at low dosages.

1. Introduction

Paper pulp is attracting widespread interest in different fields thanks to its high volume, environmental-friendly origin, and potential economic profits. It has helped the paper industry to maintain its high rank among recycling industries as a combination of recycled and virgin pulp leads to suitable paper quality [1]. Nonetheless, digitization has caused less demand for paper pulp, especially in Europe and North America [2]. This reduction has resulted in initiating endeavors to transform the paper industry and find other ways to valorize paper pulp. So far, the valorization methods have been limited to applications such as manufacturing fibrous insulation in buildings [3], producing bitumen thickener in asphalt [3], or producing energy by incineration [3,4]. In a quest for a desirable industry for valorization, the cement and concrete industry would be a right candidate, because of both enormous volume produced worldwide annually (4.1 and 25 billion tons for cement and concrete, respectively [5,6]) and the big admixture market (estimated to be $38 billion by 2024 [7]).

Currently, as detailed in Table 1, one way to valorize wood-based pulp is to incorporate it as a reinforcing agent in cement

Abbreviations: *BFS*, Blast furnace slag; *BM*, Bingham model; *CF*, Cellulose fiber; *CMF*, Cellulose microfiber; *CNF*, Cellulose nanofiber; *HB*, Herschel-Bulkley; *HBM*, Herschel-Bulkley model; *HPP*, High-energy milled paper pulp; *LPP*, Low-energy milled paper pulp; *MB*, Modified Bingham; *MBM*, Modified Bingham model; *MM*, MasterMatrix DSC 100; *MVD*, Minimum VMA demand to stop flow; *MWD*, Minimum water demand to initiate flow; *OPC*, Ordinary Portland cement; *PCE*, Polycarboxylic ether; *PP*, Paper pulp; *PVA*, Polyvinyl alcohol; *REF*, Reference; *RVD*, Relative VMA demand to decrease fluidity; *RWD*, Relative water demand to increase fluidity; *SP*, Superplasticizer; *VMA*, Viscosity modifying admixture.

* Corresponding author at: Department of the Built Environment, Eindhoven University of Technology, P.O. Box 513, 5600 MB Eindhoven, The Netherlands.
E-mail address: q.yu@bwk.tue.nl (Q. Yu).

https://doi.org/10.1016/j.conbuildmat.2020.120660
0950-0618/

Nomenclatures

c	curvature parameter of the modified Bingham model [Pa·s^2]	σ_D	dynamic yield stress of Bingham model [Pa]
K	consistency factor of the Herschel-Bulkley model	σ_0	yield stress of the Herschel-Bulkley model [Pa]
n	flow index of the Herschel-Bulkley model	η_B	plastic viscosity of the Bingham model [Pa·s]
$\dot{\gamma}$	shear rate [s^{-1}]		
σ	shear stress [Pa]		

Table 1
An overview of the research on applying wood-based pulp in cement composites.

Authors	Recipe		Properties tested	
	Binder	Fibril types	Pulp %	Application
Correia et al. 2018 [8]	OPC*	Bamboo pulp + CNF‡	8%	Reinforcement of extruded cement paste
Campello et al. 2016 [9]	OPC*	Bamboo pulp	6%	Reinforcement of cementitious composites
Khorami et al. 2016 [12]	OPC*	Waste kraft pulp	8%	Asbestos replacement in fiber cement board
Shokrieh et al. 2015 [18]	OPC* + Bentonite	PVA† + Cellulose pulp	3% to 7.5%	Reinforcement of cement composite sheets
Ballesteros et al. 2015 [20]	OPC*	Pine and eucalyptus pulp	5%	Reinforcement in cementitious matrices
Claramunt et al. 2015 [19]	OPC*	Conventional pulp + Nanofibrillated pulp	8%	Reinforcement in cement mortars
Hosseinpourpia et al. 2014 [26]	OPC*	Waste sulfite pulp	5% to 15%	Reinforcement in cementitious composites
Tonoli et al. 2013 [13]	OPC*	Isocyanate-treated eucalyptus kraft pulp	5%	Reinforcement in cement composites
Khorami & Ganjian 2013 [14]	OPC*	Kraft pulp	1–14%	Flexural improvement of cement composites
Mármol et al. 2013 [23]	OPC* + Gypsum	Softwood pulp (Pinus)	9%	Reinforcement in cementitious composites
Jongvisuttisun et. al. 2012 [27]	OPC*	Eucalyptus pulp	7.5% to 15%	Internal curing
Mezencevova et al. 2012 [28]	OPC*	Thermomechanical pulp (TMP)	5%	Internal curing
Tonoli et al. 2010 [21]	OPC*	Eucalyptus pulp	5%	Reinforcement of cementitious materials
Tonoli et al. 2010 [22]	OPC*	Eucalyptus and pine kraft pulp	10%	Reinforcement of cement composites
Mohr et al. 2007 [15]	OPC* + Pozzolans	Kraft pulp	4%	Reinforced cement-based materials
El-Ashkar et al. 2007 [16]	OPC*	Kraft pulp	1.2% and 2%	Reinforced cement mortars
Tonoli et al. 2007 [24]	OPC*	Sisal pulp	4.7%	Reinforced cement composites
Rodrigues et al. 2006 [10]	OPC* + Pozzolan	Bamboo pulp	8%	Reinforced cement composites
Mohr et al. 2006 [17]	OPC*	Kraft pulp	4%	Reinforced cement composite
Savastano Jr. et al. 2003 [25]	OPC* and BFS[3]	Sisal pulp	8%	Reinforced cement
Coutts et al. 1994 [11]	OPC*	Bamboo pulp	10%	Reinforced cement composite

* Ordinary Portland Cement; ‡ Cellulose Nano Fiber; [3]Blast Furnace Slag; † Polyvinyl alcohol.

composites. For example, there has been extensive research on applying bamboo pulp [8–11], kraft pulp [12–17], cellulose pulp [18,19], Pine and eucalyptus pulp [20–22], pinus pulp [23], sisal pulp [24,25], and waste pulp [26] in cement composites as a reinforcement. Another way to valorize wood-based pulp is to utilize it as an internal curing agent for cement composites [27,28]. Pulp dosages of up to 15% weight of cementitious materials have been reported for both applications. However, little attention has been paid to the wood-based pulps.hierarchical and hydrophilic characteristics of the wood-based pulp as a route to make highly effective concrete additives.

As shown in Fig. 1, the paper pulp has a hierarchical structure [29] in which macro fibers consist of microfibers where the latter are also made up of nanofibers. Such a hierarchical structure and hydrophilic properties can be used to form a hypothesis that different levels of fineness of the same source of paper pulp would be obtained by mechanical milling, resulting in exposing and spreading hydrophilic fibers at different levels of the hierarchy to produce various highly effective versatile VMAs. VMAs are usually water-soluble natural, semi-synthetic, or synthetic admixtures used to adjust the rheological behavior of cement composites [30]. Their application includes a wide variety of uses such as self-consolidating concrete [31], under-water concrete [32], Ultra-high performance concrete (UHPC) [33–35], cement asphalt mixtures [36], pumpable concrete and shotcrete [37,38], oil-well concrete [39] and 3D printing concrete [40]. Different VMAs have various effects on the rheological behavior of cement composites. Hence, characterizing the added value of a new source of VMA is of vital importance.

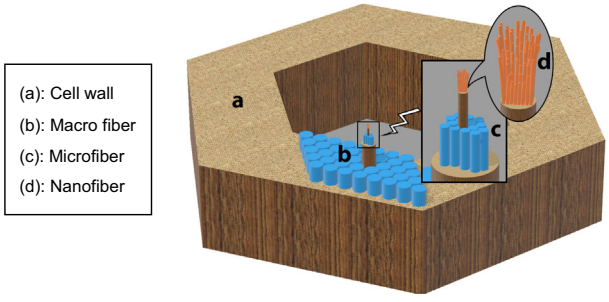

Fig. 1. The schematic hierarchical arrangement of fibers in paper pulp.

This study examines milled paper pulp as an innovative viscosity modifying admixture for cement composites. Milled paper pulp differs from most polymeric VMAs in that in the first place, it is not water-soluble. In the second place, it has two pivotal geometric parameters, namely the diameter and length of fibers. Insolubility in water makes the size and morphology of milled paper pulp significantly influential on the rheological adjustment performance. These characteristics would be used to manufacture versatile VMAs with different levels of viscosity-modifying properties. Besides, in addition to the rheological behavior, several substantial hardened properties of cement composites such as hydration kinetics, shrinkage, and strength rely strongly on water. Consequently, the hydrophile milled paper pulp might also affect these hardened characteristics. Furthermore, cement composites have a highly alkaline environment that might affect the structural integrity of milled paper pulp at an early age.

This study aims at filling these research gaps by a methodological approach that begins with manufacturing and characterizing milled paper pulp at two different fineness. Next, the influence of the fineness of paper pulp on the rheological properties of cement composites is characterized by different rheological models and compared to those of two commercially available VMAs, namely diutan gum and MasterMatrix. Then, the effects of the fineness of milled paper pulp on the hydration kinetics and autogenous shrinkage of cement composites are studied. Additionally, the stability of milled paper pulp at high pH is evaluated by calcium hydroxide treatment. Finally, Welch's ANOVA and Games-Howell post hoc tests are utilized to investigate the influences of milled paper pulp fineness on the compressive and flexural strengths of cement mortars.

2. Materials and methods

2.1. Materials

The current investigation involved analyzing the influences of fineness of paper pulp on the fresh and hardened properties of cement grouts. Milled paper pulp was manufactured at two different fineness by mechanical milling of the same source of paper pulp at different energy levels at Sappi (the Netherlands) and is referred to as low-energy milled paper pulp (LPP) and high-energy milled paper pulp (HPP) in this study. In order to characterize the fiber length characteristics after processing, according to ISO 16065:2 [41], a Lorentzen & Wettre Online Fiber Tester device was utilized. This device reports fiber size distribution by classifying it into three types of course, fine, and ultra-fine fibers, based on the range of their dimensions, as illustrated in Fig. 2 and listed below:

- Coarse fibers: $(length > 200\mu m)$;
- Fine fibers: $(length > 100\mu m)$ OR$(length < 100\mu mANDwidth + 0.35 \cdot length > 50)$
- Ultra-fine fibers: $(length < 100\mu mANDwidth + 0.35 \cdot length < 50)$

The data in Fig. 2 suggest that more than half of the low-energy milled paper pulp (LPP) consisted of coarse fibers, whereas around 85% of the high-energy milled paper pulp was made up of ultra-fine fibers. Mid-range fine fibers constituted 10.8% and 16.7% of

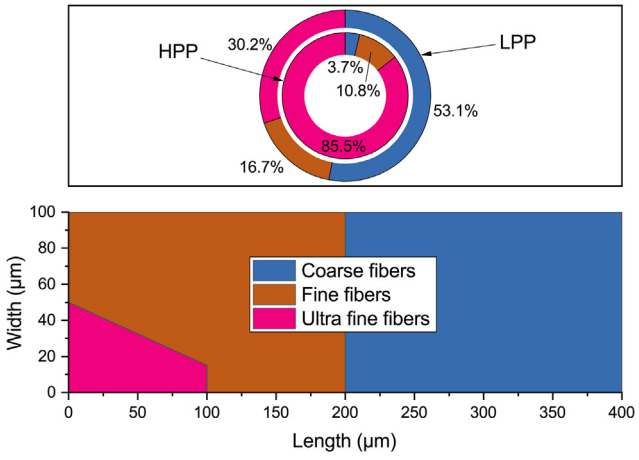

Fig. 2. Fiber length characteristics of LPP and HPP after processing: (below) the definition of ultra-fine, fine, and coarse fibers in Lorentzen & Wettre Online Fiber Tester device analysis; (above) Average weight percentages of different fiber dimensions in LPP and HPP, measured and classified by the same device.

LPP and HPP, respectively. It should be pointed out that LPP and HPP were prepared as aqueous suspensions at concentrations of 3% and 1%, respectively. As a consequence, the amount of free water was compensated in all mixture calculations.

Fig. 3 highlights the size and morphology differences between LPP and HPP in the vicinity of cement particles. Both samples were freeze-dried and scanned by a Phenom Pharos Desktop SEM from Thermo Fisher Scientific at a scale close to the median particle size of the cement utilized in this study (14 μm). The LPP consisted of fibrils of micro-size containing integrated filaments. Conversely, in HPP, microfibers were opened and flattened because of high mechanical energy, and nanofibers were exposed and spread in planes. These SEM observations are in line with the data obtained from the L&W Fiber Tester analysis in Fig. 2, as both observations confirmed higher percentages of ultra-fines in HPP.

The cement CEM I 52.5 R, provided by ENCI (the Netherlands), was used to compare and contrast the viscosity modifying performance of LPP and HPP in cement grouts. The CEM I 52.5 R is an ordinary Portland cement with a high specific surface area (Blaine of ca. 527 m^2/kg [42]) and early strength (30 MPa at one day [42]). It is appropriate for applications like shotcreting and grouting. The chemical composition of CEM I 52.5 R, identified by X-Ray Fluorescence and its particle size distribution, measured by Malvern Mastersizer 2000 particle size analyzer are detailed in Fig. 4.

A polycarboxylic ether-based superplasticizer (SP) with a solid content of 35% was utilized to disperse cement particles. The dosage of SP was calculated as the ratio of the weight of its solids to that of the binder. Neat cement grout, with no VMA, was prepared and used as the reference mixture (REF) in the study. Two commercially available high-performance VMAs, diutan gum and MasterMatrix DSC 100 (MM), were used to investigate the rheology adjustment performance of LPP and HPP. The MasterMatrix DSC 100, manufactured by BASF, was an aqueous solution of a high-molecular-weight synthetic copolymer with a recommended dosage between 0.1% and 1.0 % by weight of the binder, by the manufacturer.

2.2. Experimental methodology

2.2.1. Effects of milled paper pulp fineness on rheological behavior

A high shear mixing procedure was used to prepare all the cement grouts to not only study grouts but also provide a paste with comparable rheological properties to that of concrete from which aggregates had been removed [43]. The mixing procedure started with mixing cement with water, SP, and VMA in a double-wall mixing bowl connected to a bath thermostat at 800 rpm for 1 min at 23 °C. Then, the mixer was stopped and scraped with a spatula for 30 s. Next, the mixer was started at 2000 rpm, and the materials were mixed for another 2 min. After stopping the mixer and scraping the bowl for 30 s, the mixing was continued at the same angular velocity for 1 min. Finally, cement grouts were placed in the rheometer, and ten minutes after the cement came into contact with water, the rheometer was started to study the flow behavior. The rheometer was an Anton Paar 501 device equipped with a Peltier Plate temperature control system to keep the temperature steady at 23 °C in all the experiments. A concentric cylinder geometry consisting of a serrated bob and cup was used to avoid wall slip. All the samples were preconditioned for one minute with a shear rate of 50 s^{-1} before starting the measurements. Subsequently, a shear rate sweep was performed consisting of six one-minute steps at shear rates of 100 s^{-1}, 80 s^{-1}, 60 s^{-1},40 s^{-1}, 20 $s^{-1}$and 10 s^{-1}, respectively. In view of the fact that cement grouts showed thixotropic behavior, the shear stresses at the end of each one-minute step were recorded and used in rheological models. The recipes of the grout mixtures are shown in Table 2.

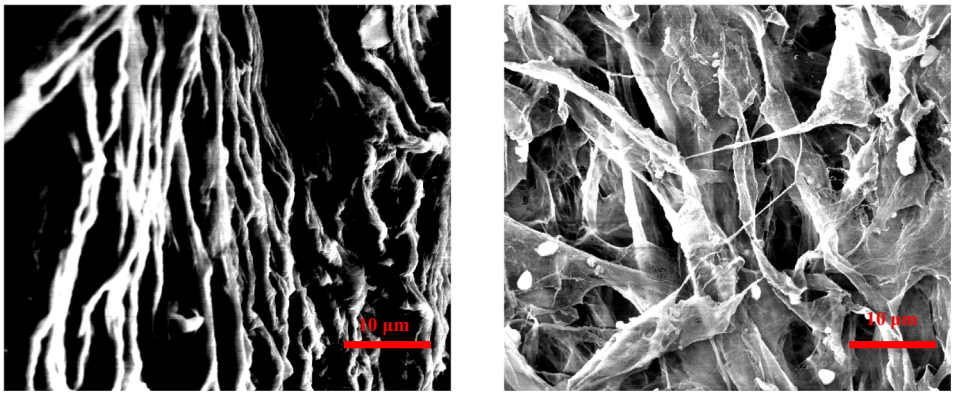

Fig. 3. The micrographs of milled paper pulp at different fineness: (left) LPP; (right) HPP.

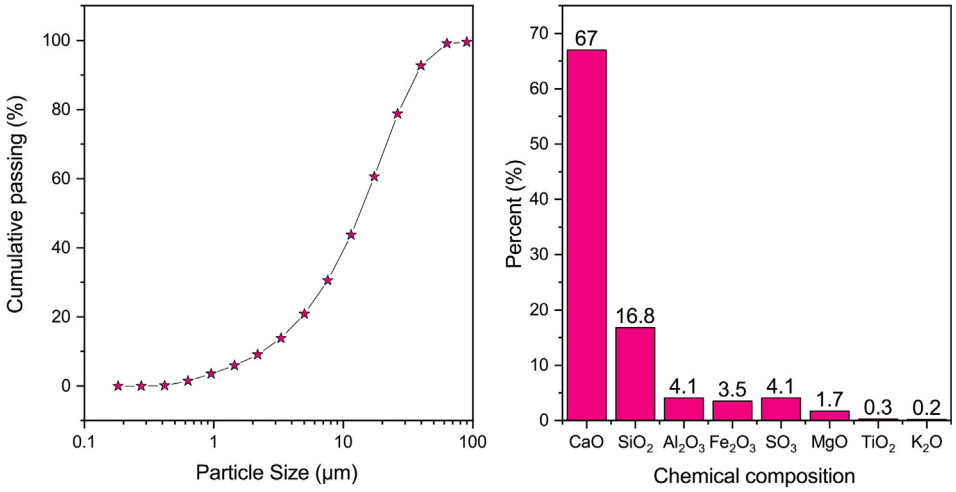

Fig. 4. Physical and chemical properties of the cement CEM I 52.5R: (left) Cumulative particle size distribution; (right) chemical composition.

As mentioned before, the superplasticizer (SP), HPP, and LPP were aqueous suspensions at the concentrations of 35%, 3%, and 1%, respectively. For the reason that the amount of free water was compensated in all the mixtures, the dosages shown in Table 2 present the dosage of their solids. In other words, LPP and HPP at their maximum dosage of 0.12% in Table 2, were aqueous suspensions at the dosages of 4% and 12% of cement weight, respectively. These dosages were selected based on our previous studies [44] and technical literature [39,45]. Another reason for opting for these dosages was to test similar dosages of LPP and HPP with those of diutan gum and the maximum recommended dosage of MasterMatrix.

In order to quantify viscosity-modifying performances of VMAs, the Bingham model (BM) and Herschel-Bulkley model (HBM) were used. The Bingham model is expressed as

$$\sigma = \sigma_D + \eta_B \dot{\gamma} \tag{1}$$

with σ the shear stress, σ_D the dynamic yield stress, η_B the plastic viscosity, and $\dot{\gamma}$ the shear rate. This model is widely used to describe the rheological behavior of cementitious materials [46] and can be employed to characterize the viscosity modifying influence of VMAs.

The Herschel-Bulkley model is a combination of the Bingham and power-law models and has the form

Table 2
Recipe of cement grouts modified with different viscosity modifying admixtures, namely MasterMatrix, diutan gum, LPP, and HPP. The dosages of SP, diutan gum, LPP, and HPP are shown as the ratio of the weight of solids to that of the cement. The dosage of MasterMatrix is demonstrated as the weight of the liquid synthetic copolymer to that of the cement.

Mix	w/c	SPdosage (%)	MasterMatrixdosage (%)	Diutan gumdosage (%)	LPPdosage (%)	HPPdosage (%)
REF	0.4	0.175%	0	0	0	0
MM5	0.4	0.175%	0.5%	0	0	0
MM10	0.4	0.175%	1.0%	0	0	0
D4	0.4	0.175%	0	0.04%	0	0
D8	0.4	0.175%	0	0.08%	0	0
D12	0.4	0.175%	0	0.12%	0	0
LPP4	0.4	0.175%	0	0	0.04%	0
LPP8	0.4	0.175%	0	0	0.08%	0
LPP12	0.4	0.175%	0	0	0.12%	0
HPP4	0.4	0.175%	0	0	0	0.04%
HPP8	0.4	0.175%	0	0	0	0.08%
HPP12	0.4	0.175%	0	0	0	0.12%

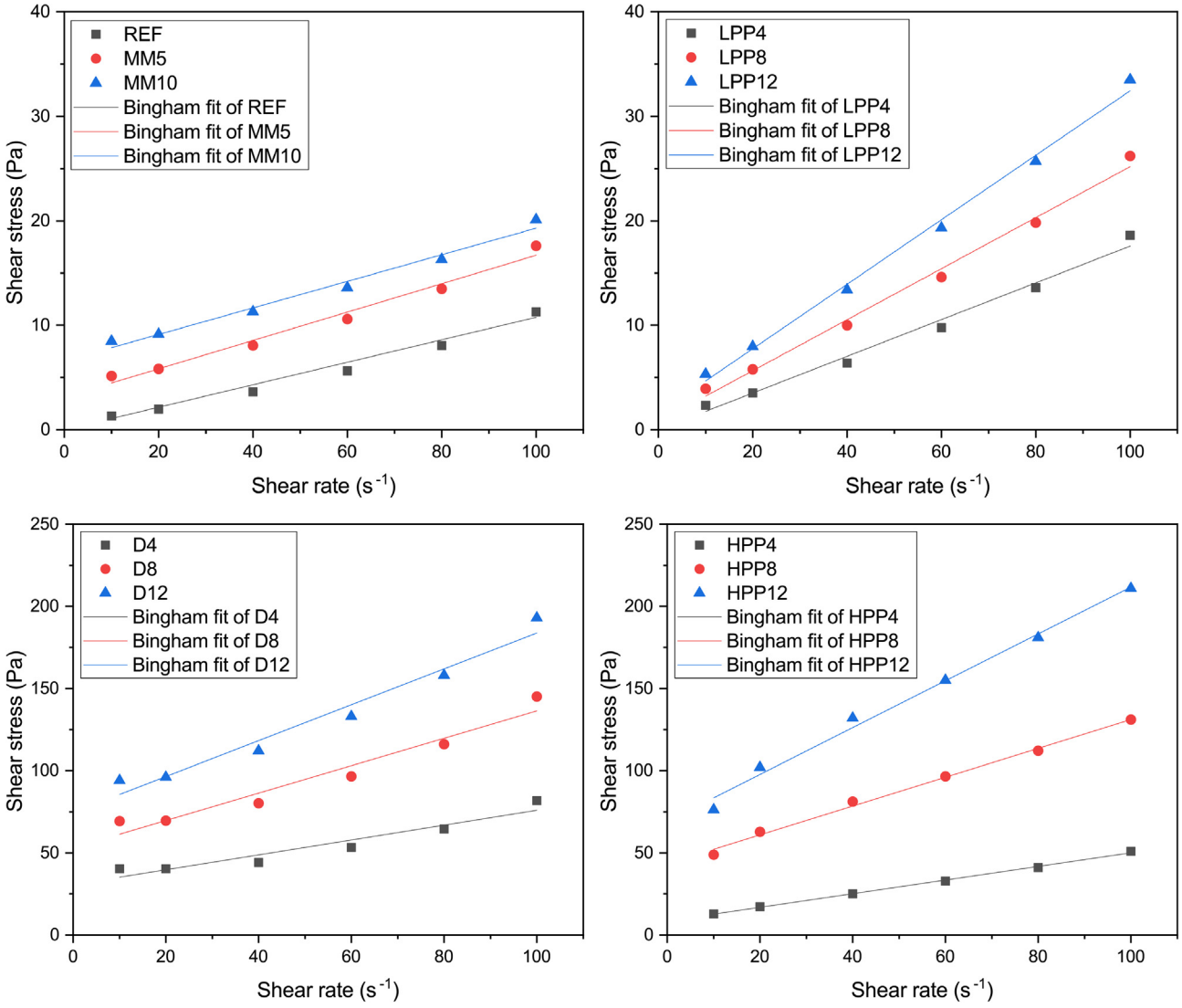

Fig. 5. Rheological data and Bingham fits of grouts with different viscosity-modifying admixtures (REF: reference; MM: MasterMatrix; D: diutan gum; LPP: Low-energy milled paper pulp, and HPP: High-energy milled paper pulp).

$$\sigma = \sigma_0 + K\dot{\gamma}^n \quad (2)$$

with σ_0 the yield stress of this model, K the consistency factor, n the flow index, and σ and $\dot{\gamma}$ as used previously.

2.2.2. Effects of milled paper pulp fineness on hydration kinetics

The hydration kinetics of the cement grouts were measured using a TAM Air isothermal calorimeter, according to ASTM C1679 [47]. First, all the samples were mixed externally and were

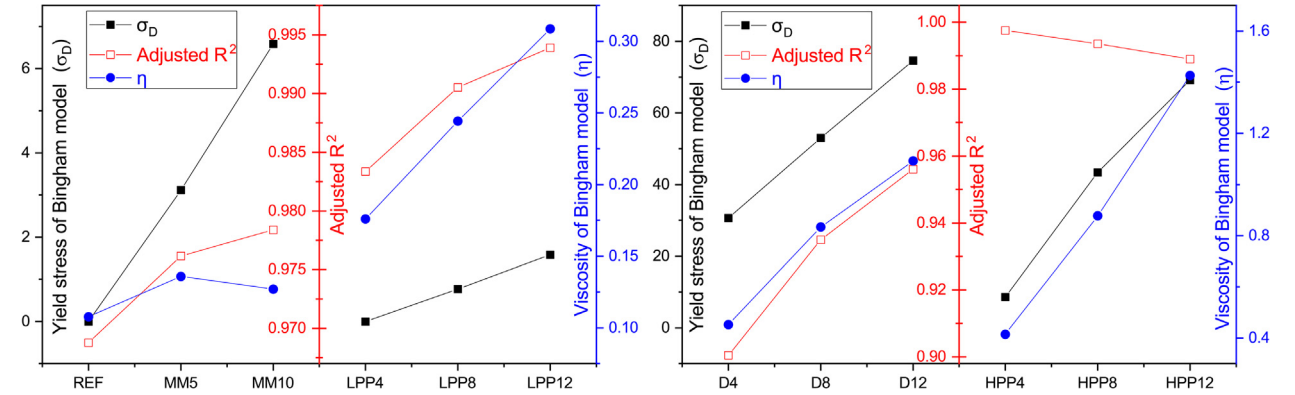

Fig. 6. The Bingham model parameters of grouts with different viscosity-modifying admixtures (REF: reference; MM: MasterMatrix; D: diutan gum; LPP: Low-energy milled paper pulp, and HPP: High-energy milled paper pulp).

transferred into glass ampoules and sealed. Then, they were loaded into the calorimeter to measure the heat flow for seven days, with a set temperature of 20 °C. The hydration kinetics results were evaluated by comparing the graphs of normalized thermal power as a function of time, according to ASTM C1679 [47]. The mixtures REF, D8, LPP8, HPP8, and MM10 of Table 2, were utilized in hydration kinetics studies, with the mere difference that superplasticizer dosages in all the samples were raised from 0.175% to 0.28% (i.e., the dosage of the aqueous solution of superplasticizer was raised from 0.5 to 0.8) to ease inserting grouts into the ampoules.

2.2.3. Effects of milled paper pulp fineness on shrinkage

The autogenous shrinkage of cement grouts was measured according to ASTM C1698 [48] to investigate the water stabilization performance of the studied additives and possible influences on volume change of cement composites. This standard test method utilizes a dilatometer bench to measure the length change of corrugated tubes, filled with grouts under constant temperature. Three replicate samples were made, and the measurements started after the final setting time of the grouts. The final setting time was determined, according to ASTM C191 [49]. The corrugated plastic tubes had a length of 420 ± 5 mm and an outer diameter of 29 ± 0.5 mm. All the samples and measurement devices were stored in a climate chamber at 23 ± 1 °C. Similar mixtures as those used in hydration kinetics studies were utilized for autogenous shrinkage experiments.

2.2.4. Simulated aging of milled paper pulp

In order to simulate the highly alkaline environment of the binder, a saturated solution of calcium hydroxide ($Ca(OH)_2$) with a pH of 12.4 was prepared. Then, HPP and LPP were added to the solution and stored for 20 days. Next, the samples were dried in a freeze dryer (Alpha 1 – 4 LD plus from Christ) using the following settings:

- Ice condenser = -57 °C
- vacuum < 1 bar
- t = 48 h

Finally, a Perkin Elmer Frontier Fourier Transform Infrared Spectrometer (FTIR) equipped with a GladiATR diffuse reflectance (ATR) module was used to record the spectra of the freeze-dried samples before and after simulated aging. Eight scans were

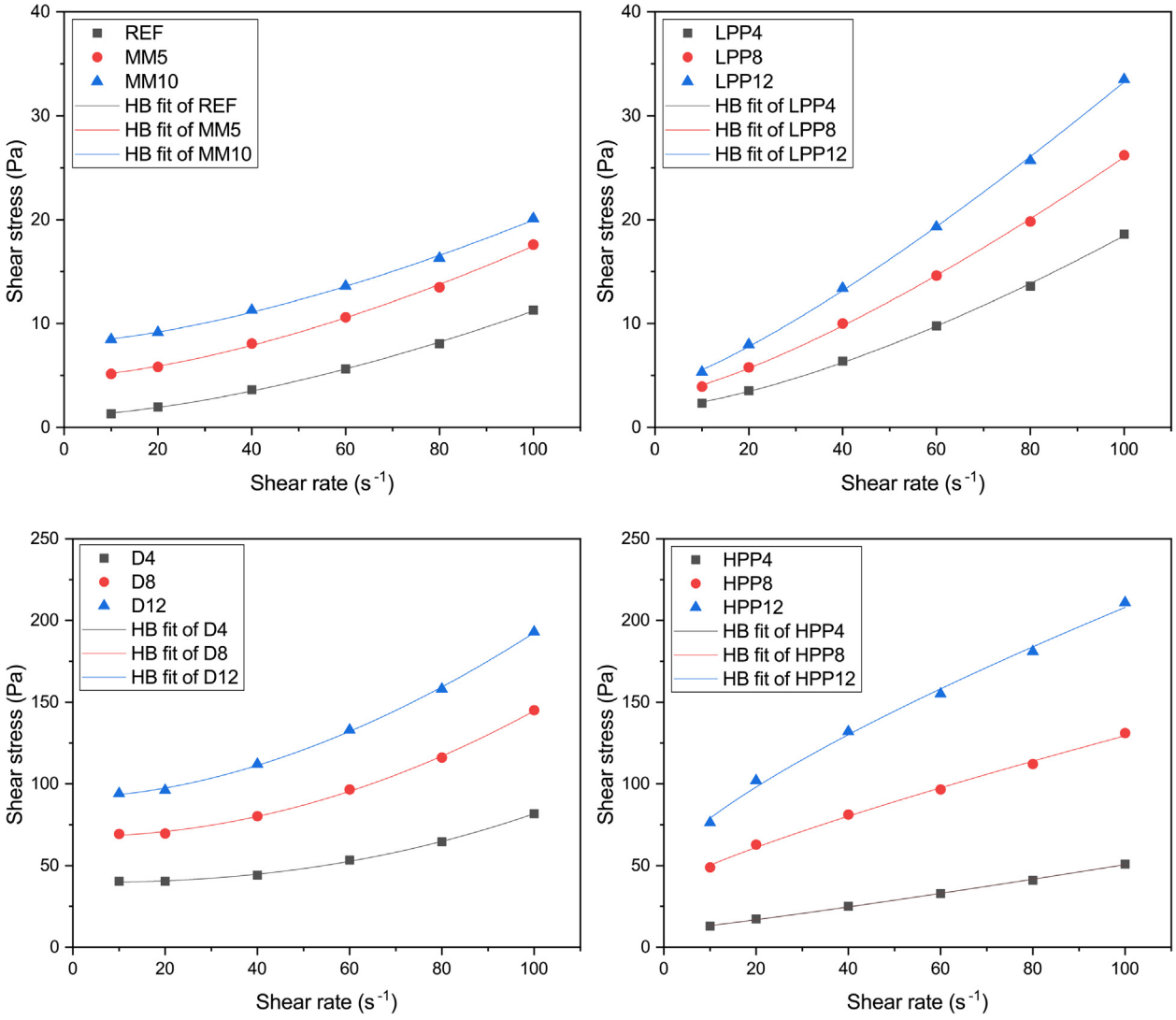

Fig. 7. Rheological data and Herschel-Bulkley fits of grouts with different viscosity-modifying admixtures (REF: reference; MM: MasterMatrix; D: diutan gum; LPP: Low-energy milled paper pulp, and HPP: High-energy milled paper pulp).

acquired with optical retardation of 0.25 cm and a resolution of 4 cm^{-1} from the wavelength of 400 to 4000 cm^{-1}.

It should be noticed that in ATR mode, the absolute value of the area of a peak cannot be used for quantitative analysis as this method only characterizes the surface of the sample. However, a significant reduction of a peak can indicate a structural change.

2.2.5. Effects of milled paper pulp fineness on compressive and flexural strengths

Early-age flexural and compressive strengths were assessed to evaluate the possible crack-bridging and reinforcement by the fibers. All the standard mortar samples (water:cement:sand = 1:2:6) were prepared using a Hobart mixer, according to EN 196–1:2016 [44]. Cement, water, SP, and VMA were mixed at low speed (140 ± 5 rpm) for one minute. Next, the mixer was switched to high speed (285 ± 10 rpm), and mixing was continued for another 30 s. The mixer was stopped, and its walls were scraped for 30 s. Finally, after mixing for another 60 s at high speed (285 ± 10 rpm), the mortars were poured in prism specimens, 40 × 40 × 160 mm^3. The specimens were demolded 24 h after casting and were cured in water at about 21 °C before the tests. Tap water was used for curing to keep conditions as similar as possible to concrete in practice. The flexural and compressive strengths of the specimens were measured using 50 N/s and 2400 N/s as the test speeds, respectively. One-way Welch's Analysis of Variance (ANOVA) was used to evaluate the effect of VMAs on the mechanical properties of mortars. The analysis was evaluated at 5% significance level (α), considering the equality of all means as the null hypothesis (Ho) and the non-equality of all means as the alternative hypothesis (Ha). Furthermore, Games-Howell post hoc tests were used to compare the mean differences between VMAs pairs at different ages.

3. Results

3.1. Effects of milled paper pulp fineness on rheological behavior

As mentioned previously, the flow behavior of the grouts was characterized by two rheological models, namely the Bingham model and the Herschel-Bulkley model. The rheological data and Bingham fits of the grouts are demonstrated in Fig. 5. In general, all the viscosity-modifying admixtures increase the shear stress at similar shear rates, compared to the reference. The more the dosage of the VMA, the higher the value of the shear stress. Furthermore, the range of shear stress of the grouts containing MasterMatrix and LPP is comparable to each other ($\sigma < 40$). Similarly, although the shear stress in grouts incorporating HPP or diutan gum is several times higher than that in grouts having LPP and MasterMatrix (MM) at similar shear rates, the range of shear stress of the former grouts is comparable to each other ($\sigma < 250$).

In order to quantify these differences and similarities, the parameters of the Bingham model, namely dynamic yield stress and plastic viscosity, together with adjusted R^2 of the fittings, are

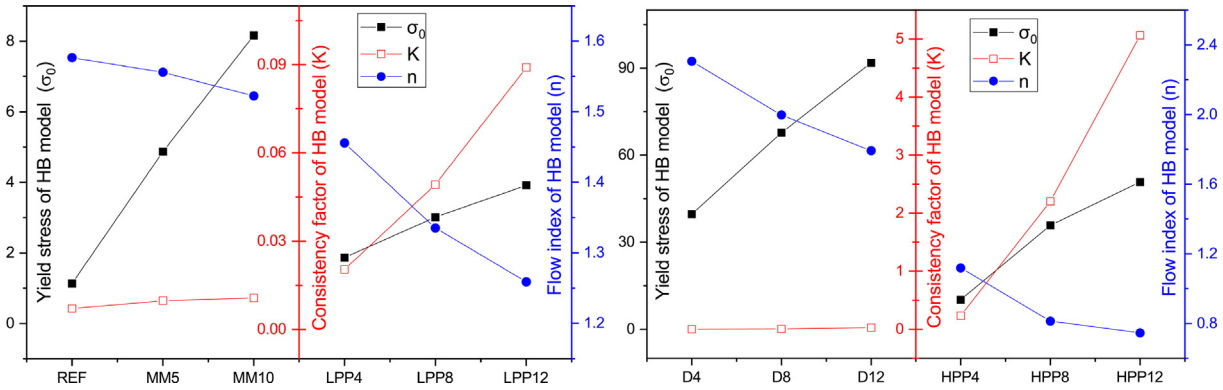

Fig. 8. Herschel-Bulkley model parameters of grouts with different viscosity-modifying admixtures (REF: reference; MM: MasterMatrix; D: diutan gum; LPP: Low-energy milled paper pulp, and HPP: High-energy milled paper pulp).

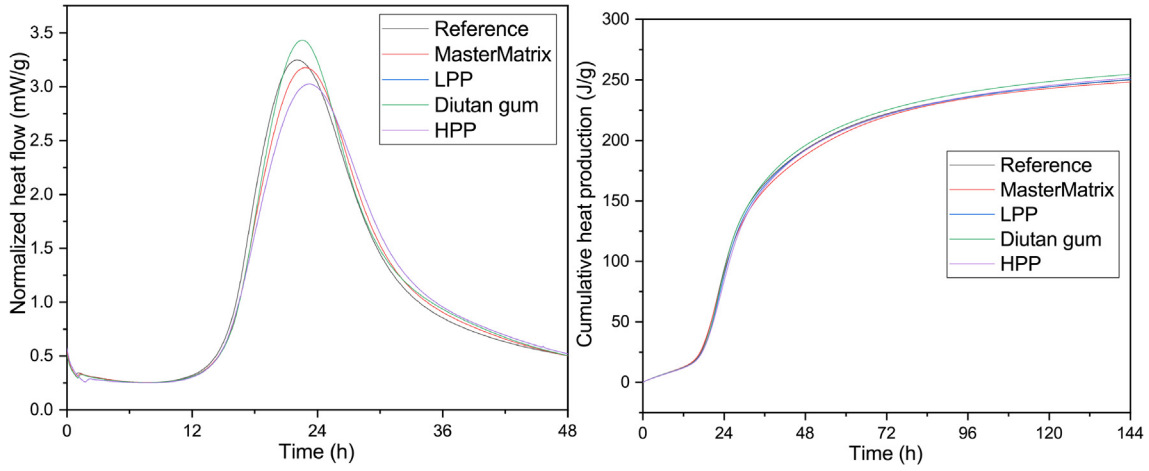

Fig. 9. Isothermal hydration profiles of HPP, LPP, and commercially-available VMAs: (left) heat flow; (right) cumulative heat release.

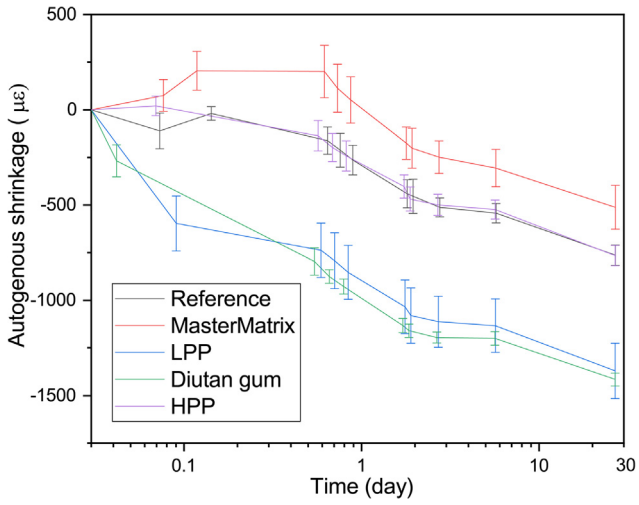

Fig. 10. Autogenous shrinkage of cement grouts with different VMAs.

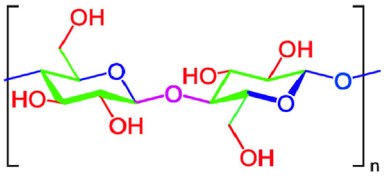

Fig. 11. Cellulose structure. The chemical functions are highlighted.

Table 3
Chemical bonds of cellulose and their respective wavelength in FT-IR spectrometry [55].

Function	Description	Wavelength (cm^{-1})
–OH	Primary and secondary alcohols	3600–3200
-O-	Ether bonds (glucose)	1205–1050 (several)
$–CH_2–$	Alkenyl bonds	2900; 1370
-O-	β-glycosidic linkage	900
H-O–H	Bonded water	1640

compared and contrasted in Fig. 6. As the range of the parameters of LPP and HPP grouts is close to those of MasterMatrix and diutan gum grouts, respectively, the rheological parameters of LPP grouts are paired with those of MM grouts. In contrast, the rheological parameters of HPP grouts are paired with those of the diutan gum grouts.

The values of the adjusted R^2 of the Bingham models for REF, LPP, and MM are more than 0.97, which confirm a strong correlation. Adding LPP to cement grouts increases the dynamic yield stress and plastic viscosity. The values of the plastic viscosity of LPP grouts at the dosages of 0.08% and 0.12% are higher than those of the MM mixtures at half maximum (0.5%) and maximum (1%) dosages, respectively. Besides, LPP increases the yield stress lower than the synthetic copolymer (MM).

Furthermore, the finer milled paper pulp (HPP) increases both yield stress and plastic viscosity more than LPP. The effect of HPP on rheological behavior is comparable to that of diutan gum. However, HPP increases plastic viscosity more than diutan gum and enhances yield stress lower than diutan gum at similar dosages. It should also be noted that the value of adjusted R^2 falls to 0.9 in the Bingham fittings of the diutan gum grouts, which can be interpreted as an indicator of nonlinear behavior. In order to elucidate these nonlinearities, the Herschel-Bulkley fits of the rheological data are demonstrated in Fig. 7. All the flow curves could be well-captured by this model (Adjusted R^2 greater than 0.99). The parameters of the Herschel-Bulkley fits of the grouts, namely yield stress, flow index, and consistency factor are compared and contrasted in Fig. 8.

Adding MasterMatrix (MM) or LPP increases the HB yield stress. However, MM increases the HB yield stress at half its maximum dosage (0.5%), more than LPP at the maximum dosage used in this study (0.12%). Although both K and n parameters of the HB model are nothing more than fitting parameters [50], both MM and LPP keep the flow index at the range of 1.2 to 1.6. Fig. 8 also demonstrates that diutan gum increases the HB yield stress more than HPP at similar dosages. Furthermore, adding HPP changes the sign of the flow index, making the curvature negative (shear-thinning behavior).

3.2. Effects of milled paper pulp fineness on hydration kinetics

A comparison of the effects of milled paper pulp fineness (LPP and HPP) with two commercially-available VMAs on hydration kinetics is illustrated by the isothermal hydration profiles in Fig. 9.

An isothermal hydration profile is a useful tool to compare the rate of hydration over time and can be used to calculate the thermal indicator of setting time, which is the hydration time to reach a thermal power of 50% of the maximum value of the main peak [47]. Studies have shown that some wood-based pulp may deteriorate hydration kinetics due to water-soluble sugars [51,52]. The effect of MasterMatrix, diutan gum, LPP, and HPP on both thermal indicator of setting time and hydration kinetics are insignificant. This negligible influence may be attributed to the very low dosages of the admixtures needed for modifying the rheological properties.

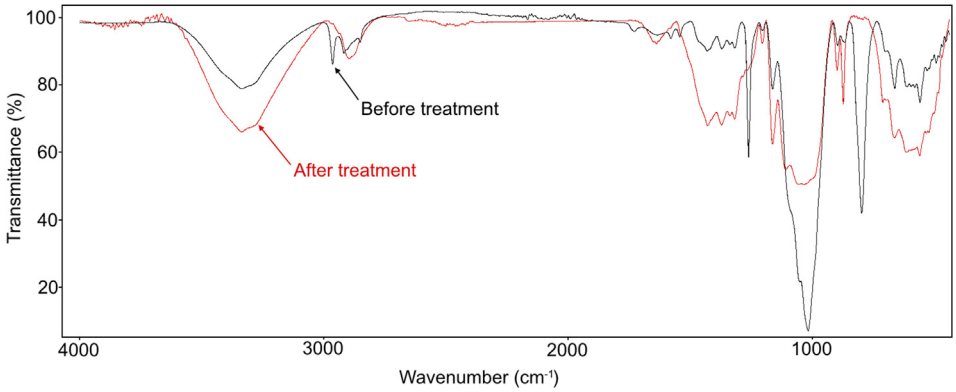

Fig. 12. FTIR spectra of LPP before (in black) and after (in red) simulated aging. (For interpretation of the references to color in this figure legend, the reader is referred to the web version of this article.)

The cumulative hydration heat curves also display a very similar degree of hydration heat for all VMAs in six days.

The peak of all isothermal hydration profiles occurs at around 24 h. This retarding behavior is due to PCE superplasticizer, incorporated in all the mixtures. The mixture having diutan gum has a slightly higher hydration peak. This result confirms the findings by Ciobanu et al. [53], where diutan gum increases the calcium hydroxide content and hydration degree that can be attributed to the low charge density of diutan gum and its tendency to adsorb out of mixing water and onto cement hydration products [54]. These studies [53,54] have also shown that these characteristics lead to lower early-age compressive strength in mixtures containing diutan gum and are discussed in Section 4.

3.3. Effects of milled paper pulp fineness on shrinkage

The effects of the fineness of milled paper pulp (HPP and LPP) on the autogenous shrinkage of the mixtures are compared with those of the commercially-available VMAs in Fig. 10. As the rate of autogenous shrinkage is higher at an early age, time is shown in logarithmic scale. Diutan gum increases the autogenous shrinkage of cement grout and doubles it after 28 days. The influence of LPP on autogenous shrinkage is similar to that of diutan gum, both increasing its value. By contrast, HPP does not affect the autogenous shrinkage of mixtures, and its value of shrinkage remains similar to that of the reference. The different influence of HPP and LPP on shrinkage may be attributed to the morphology and size differences in LPP and HPP, as previously shown in Fig. 2 and Fig. 3.

3.4. Simulated aging of milled paper pulp

Paper pulp consists of cellulose, which has glucose units linked by an ether bond named β-glycosidic linkage. Different parts of the structure can be characterized by FT-IR, as shown in Fig. 11, where four different cellulose parts can be distinguished. The primary and secondary alcohols of the glucose units are shown in red color. The alkenyl bonds forming the cyclic structure of the glucose (and a part of the secondary alcohols in the equatorial position) are shown in green color. The ether bond in the glucose unit and the β-glycosidic linkage between two glucose units are shown by blue and purple. Moreover, as cellulose is a hygroscopic material, bonded water can also be attached to the alcohol groups. Table 3 sums up the corresponding bonds as characterized by FT-IR.

The FT-IR analyses of LPP and HPP, before and after simulated aging in an alkaline solution, are shown in Fig. 12 and Fig. 13, respectively. Table 4 summarizes the results by assigning characteristic peaks to their corresponding function for each sample. Before and after simulated aging, the spectra of LPP are quite similar, with the presence of cellulose characteristic bonds such as ν_{OH}, $\nu_{CH,}$ and ν_{C-O-C}. Nevertheless, some structural changes are noticeable with the disappearance of peaks at 1250 cm^{-1} and 800 cm^{-1}, which correspond to benzoate ether and C–C bonds, respectively. As these bonds are not present in the cellulose, it indicates the presence of impurities at the surface of the LPP, which are removed after simulated aging. With HPP, the first observation is the presence of water after aging, with broad bands at 1634 and 3320 cm^{-1} due to the storage conditions. The two spectra are comparable except the significant reduction of the peak at 873 cm^{-1}, indicating some fragmentation of the β-glycosidic bond in the cellulose. On the whole, both HPP and LPP show good stability in a highly alkaline environment for a long duration (here, 20 days), and the cellulose structure remains undamaged.

3.5. Effects of milled paper pulp fineness on compressive and flexural strengths

The influences of different VMAs on the average compressive strengths of mortars at 1, 7, and 28 days are demonstrated in Fig. 14. As mentioned previously, in order to elaborate on these influences, Welch's analysis of variance is applied. Welch's tests

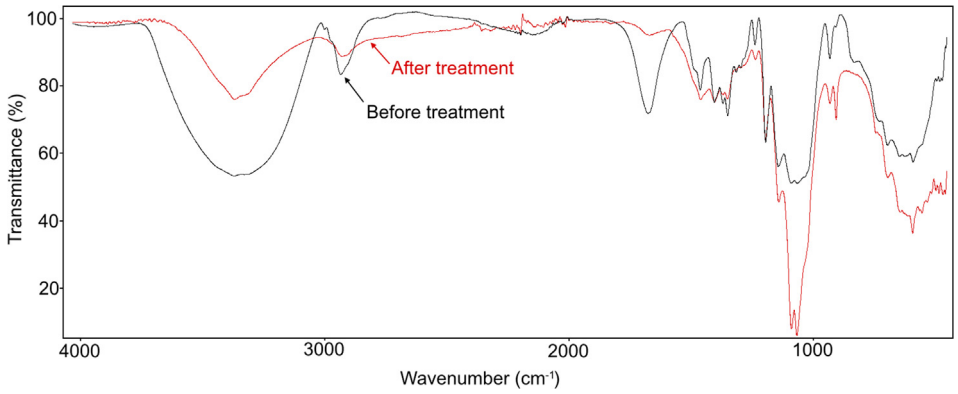

Fig. 13. FT-IR spectra of HPP before (in black) and after (in red) simulated aging. (For interpretation of the references to color in this figure legend, the reader is referred to the web version of this article.)

Table 4
Main FTIR absorption band assignments.

Wavenumber (cm^{-1})	LPP before	LPP after	HPP before	HPP after
ν_{OH}*	3333	3339	3335	3334
ν_{CH}*	2962–2915	2920–2851	2900	2896
H_2O absorbed	–	1636	–	1645
δ_{CH2}‡	1429	1428	1428	1424
δ_{CH}‡, ν_{COO}*	1369	1370	1370	1375
ν_{C-O}*, δ_{OH}‡	1161	1161	1160	1161
ν_{C-O}*	1048–1015	1033	1053–1034	1060–1031
ν_{C-O-C}*	894–872	897–872	896–875	899

* ν: bending vibration; ‡ δ: stretching vibration.

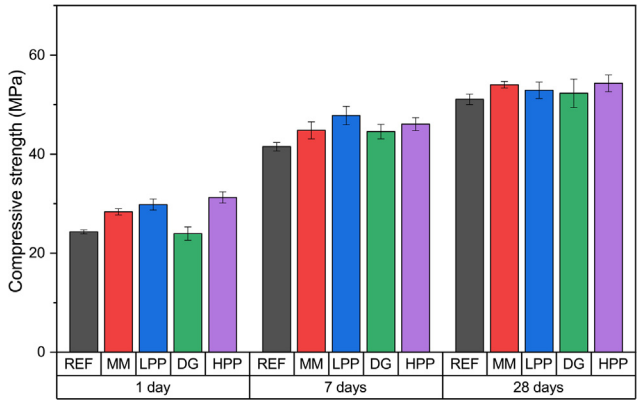

Fig. 14. Influence of different VMAs on the average compressive strengths of mortars at 1, 7, and 28 days. Error bars show the standard deviation. (REF: reference; MM: MasterMatrix; D: diutan gum; LPP: Low-energy milled paper pulp, and LPP: High-energy milled paper pulp).

of the VMAs' influence on the 1-day, 7-day, and 28-day compressive strengths of mortars are listed in Table 5.

The standard deviations of the strengths of the mortars have significant differences, which show that the choice of Welch's ANOVA over Fisher's ANOVA is reasonable. Welch's tests of the mean compressive strengths at all ages have p-values<0.05. This fact reveals that the differences in the average 1-day, 7-day, and 28-day compressive strengths of some mortars are significant. The high predicted R^2 (87.64%) in Welch's tests of the 1-day compressive strengths shows that the model generates robust predictions for new observations. Although the predicted R^2 of 7-day strengths is 56.32%, which shows a fairly strong correlation, it falls to 6.79% for 28-day average strengths, which reveals that at this age, the model generates imprecise predictions for new observations and should not be used to make generalizations beyond the sample data. This low predicted R^2 can be attributed to the small sample size (N = 6).

Games-Howell post-hoc test results are shown in Fig. 15. All of the confidence intervals of the pairs having the reference, do not

Table 5
Welch's analysis of variance (ANOVA) of the effect of VMAs on the 1-day, 7-day, and 28-day compressive strengths of the mortars (CI: confidence interval for group means; DF Den: degrees of freedom for the denominator; DF Num: degrees of freedom for the numerator; N: sample size; R-sq(adj): adjusted R^2; R-sq(pred): predicted R^2; and StDev: standard deviation).

Welch's Test (1-day compressive strengths)				
Source	DF Num	DF Den	F-Value	P-Value
Factors (VMAs)	4	11.8218	85.70	0.000
Model Summary				
R-sq.		R-sq.(adj.)		R-sq.(pred.)
91.42%		90.05%		87.64%
Means				
Factor	N	Mean	StDev	95% CI
LPP	6	29.832	1.113	(28.663, 31.000)
HPP	6	31.257	1.125	(30.076, 32.437)
REF	6	24.293	0.411	(23.862, 24.724)
MM	6	28.350	0.632	(27.687, 29.013)
D	6	23.957	1.335	(22.555, 25.358)
Welch's Test (7-day compressive strengths)				
Source	DF Num	DF Den	F-Value	P-Value
Factors (VMAs)	4	12.1869	19.45	0.000
Model Summary				
R-sq.		R-sq.(adj.)		R-sq.(pred.)
69.66%		64.81%		56.32%
Means				
Factor	N	Mean	StDev	95% CI
LPP	6	47.790	1.858	(45.840, 49.740)
HPP	6	46.038	1.316	(44.657, 47.420)
REF	6	41.520	0.862	(40.616, 42.424)
MM	6	44.807	1.726	(42.995, 46.618)
D	6	44.538	1.474	(42.991, 46.086)
Welch's Test (28-day compressive strengths)				
Source	DF Num	DF Den	F-Value	P-Value
Factors (VMAs)	4	11.7796	8.21	0.002
Model Summary				
R-sq.		R-sq.(adj.)		R-sq.(pred.)
35.27%		24.92%		6.79%
Means				
Factor	N	Mean	StDev	95% CI
LPP	6	52.897	1.665	(51.150, 54.643)
HPP	6	54.305	1.678	(52.544, 56.066)
REF	6	51.057	1.038	(49.967, 52.146)
MM	6	54.013	0.648	(53.333, 54.693)
D	6	52.29	2.88	(49.27, 55.31)

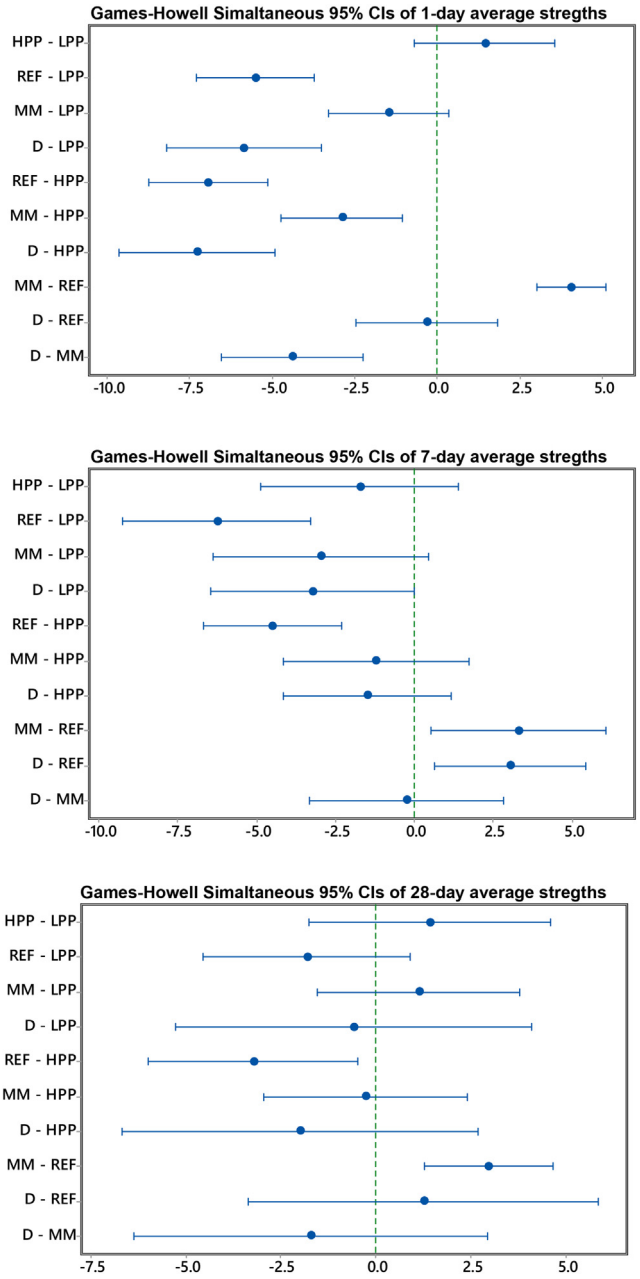

Fig. 15. Games-Howell simultaneous tests at 95% confidence intervals for differences of average 1-day, 7-day, and 28-day compressive strengths of mortars. The Intervals that do not contain zero have significantly different means.

contain zero, which means significant differences. The pairwise comparisons also exhibit that both HPP and LPP result in mortars with significant differences in average compressive strengths.

In order to elucidate these differences, Games-Howell groupings at 95% confidence at different ages are reported in Table 6. The average compressive strengths of VMAs, which are not grouped, are significantly different. HPP and LPP are grouped at all ages. This group has significantly different 1-day compressive mean strength than the reference mortar and diutan gum group. On the other hand, HPP, MM, and diutan gum constitute a group at seven days, which has significantly different average strength with the reference. These differences fade at 28 days as three groups reduce to two groups.

The average flexural strengths of mortars at 1, 7, and 28 days are demonstrated in Fig. 16. As shown in Table 7, the p-values of Welch's ANOVA of these results at all ages have values more than 0.05, the null hypotheses cannot be rejected, and there is no evidence in the data to conclude that the average flexural strengths are significantly different.

4. Discussion

The present study starts with rheological behavior analysis to assess the performance of milled paper pulp at two levels of fineness (LPP and HPP) and compares and contrasts their rheological data with those of two commercially available VMAs (MasterMatrix and diutan gum). Several rheological models have been introduced in the literature to interpret the rheological properties of cementitious materials, namely Bingham, Herschel-Bulkley, Casson, Eyring, Robertson-Stiff, De Kee, and Vom Berg models [46]. Among these, the Bingham model is more than just a fitting equation and reveals the physical differences of cement grouts. For example, plastic viscosity shows the stickiness of the material, while the critical stresses required to break the structure of cement grouts are shown by the yield stress. VMAs increase both the yield stress value and the plastic viscosity value of cement grouts [30,56]. If a graph of yield stress axis and plastic viscosity axis is made, the influence of VMAs on the rheological behavior of cement grouts can be compared [31], as shown in Fig. 17.

Such a graph is used in Fig. 18 to compare and contrast data on the influence of different levels of fineness of paper pulp on the rheological properties of cement grouts. This Figure highlights the significantly different influences of LPP and MasterMatrix on the flow parameters of cement grouts. While MasterMatrix affects the yield stress significantly, LPP mainly affects the plastic viscosity. Besides, the plastic viscosity-yield stress ratio of the HPP grouts are higher than that of diutan gum grouts at similar dosages. These insights on the performance of VMAs provide a basis for understanding the mechanism of action of paper pulp on the rheological properties of cement composites and may be used in choosing VMAs for different applications.

Furthermore, Fig. 18 shows that the influence of HPP on the flow parameters of cement grouts is a few times more significant than that of LPP at similar dosages. This difference can be attributed to the changes caused by milling to the mechanism of action of paper pulp. As previously shown in Fig. 2, while ultrafine fibers make up around 30% of LPP, their percentage rises to around 85% in HPP.

Besides, Fig. 18 demonstrates that diutan gum increases yield stress a little more than HPP and enhances plastic viscosity slightly less than HPP. The high values of yield stress and plastic viscosity in diutan gum can be attributed to the working mechanism of diutan gum in the presence of polycarboxylate ether-based superplasticizers, which is based on its high molecular weight and water immobilization [54,57].

Fig. 19 shows an SEM picture of LPP diluted in water and deposited on a silicon wafer. Item 1 shows long fibers, while Item 2 shows a stack of ultrafine fibers. The fibers are able to hold cement particles together and modify the rheological behavior of cement grouts by bridging flocculation. The magnitude of this physical mode of action can be modified by incorporating 3rd generation superplasticizers (polycarboxylic ether (PCE) based SPs) in the mixture, as these SPs cause cement particles to repel each other through a combination of electrostatic repulsion and steric hindrance [58–61] or just through steric hindrance [61–63]. Furthermore, as paper pulp fibers are hydrophilic, they can absorb and retain water resulting in a higher concentration of the matrix and a higher value of viscosity. Mechanical milling affects both bridging flocculation and swelling mechanisms of fibers and changes the performance of LPP to that of HPP as a VMA.

Table 6
Games-Howell grouping information of the 1-day, 7-day, and 28-day compressive strengths of mortars at 95% confidence. Means that do not share a letter are significantly different.

Games-Howell Pairwise comparison (1-day compressive strengths)					
Factor	N	Mean	Grouping		
HPP	6	31.257	A		
LPP	6	29.832	A	B	
MM	6	28.350		B	
REF	6	24.293			C
D	6	23.957			C
Games-Howell Pairwise comparison (7-day compressive strengths)					
Factor	N	Mean	Grouping		
LPP	6	47.790	A		
HPP	6	46.038	A	B	
MM	6	44.807	A	B	
D	6	44.538		B	
REF	6	41.520			C
Games-Howell Pairwise comparison (7-day compressive strengths)					
Factor	N	Mean	Grouping		
HPP	6	54.305	A		
MM	6	54.013	A		
LPP	6	52.897	A	B	
D	6	52.29	A	B	
REF	6	51.057		B	

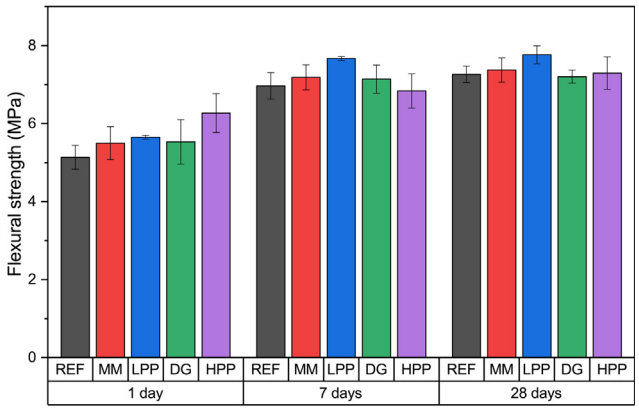

Fig. 16. Influence of different VMAs on the average flexural strengths of mortars at 1, 7, and 28 days. Error bars show the standard deviation. (REF: reference; MM: MasterMatrix; D: diutan gum; LPP: Low-energy milled paper pulp, and HPP: High-energy milled paper pulp).

The dynamic yield stress is calculated by extrapolating rheological data. Hence, although the linear Bingham model provides a basis for comparing and contrasting different VMAs based on yield stress and plastic viscosity, the value of the extrapolated dynamic yield stress diverges from its true value as nonlinearity in the rheological data rises. In these cases, the Herschel-Bulkley model gives a more realistic yield stress value as it fits nonlinear data better.

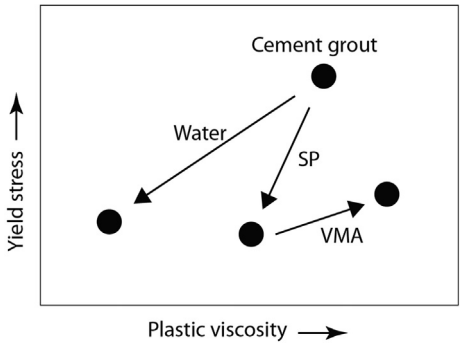

Fig. 17. Effect of adding water, superplasticizer (SP), or VMA on the Bingham yield stress and plastic viscosity of cement grout [31].

However, as this model does not give information on the viscosity of the cement grouts, comparing different VMAs with this model is difficult. In order to take this nonlinearity into account, a few researchers proposed to use a second-order polynomial model as follows

$$\sigma = \sigma_D + \eta_B\dot{\gamma} + c\dot{\gamma}^2 \tag{3}$$

with c the c-parameter, and $\sigma_D, \sigma, \dot{\gamma}, \text{and } \eta_B$ as used previously [64,65]. The modified Bingham properties are then calculated by suppressing the second-order term, which is significantly low

Table 7
Welch's analysis of variance (ANOVA) of the effect of VMAs on the 1-day, 7-day, and 28-day flexural strengths of the mortars (DF Den: degrees of freedom for the denominator; DF Num: degrees of freedom for the numerator).

Welch's Test (1-day flexural strengths)				
Source	DF Num	DF Den	F-Value	P-Value
Factors (VMAs)	4	4.11667	2.26	0.221
Welch's Test (7-day flexural strengths)				
Source	DF Num	DF Den	F-Value	P-Value
Factors (VMAs)	4	4.15687	5.65	0.057
Welch's Test (28-day flexural strengths)				
Source	DF Num	DF Den	F-Value	P-Value
Factors (VMAs)	4	4.90180	2.24	0.203

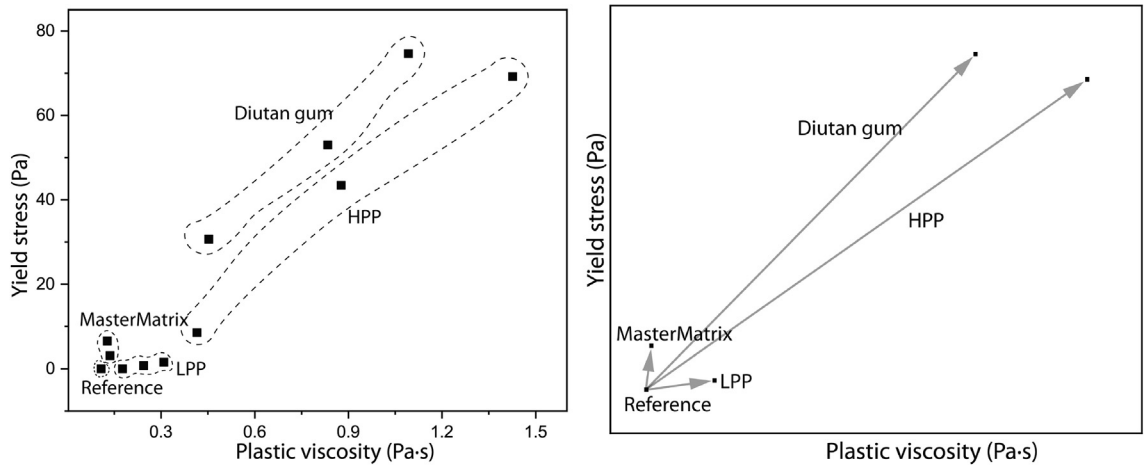

Fig. 18. Effect of different VMAs on the Bingham yield stress and plastic viscosity of cement pastes at the maximum dosage studied in this paper.

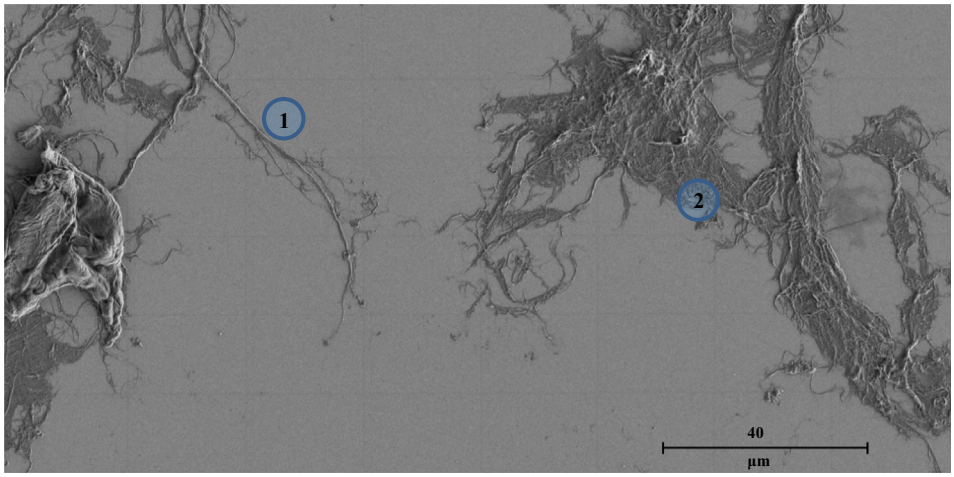

Fig. 19. SEM picture of LPP in water with ET detector; 1-long fibers, 2-small fibers (Courtesy of Sappi®).

[66]. However, if the second-order term is significant, there is no reason to be suppressed. If not, it might be erroneous to use the modified Bingham model this way, as it cannot differentiate between a material with modified Bingham properties (σ_D, η_B, c) of say (a, b, c) with another material with modified Bingham properties of (a, b, c'). Hence, this study proposes to apply the modified Bingham model, but instead of suppressing the c-parameter, utilize it to show the deviation from the Bingham model or in other words to show the nonlinearity. The c-parameters of the grouts are shown in Fig. 20. The adjusted R^2 of the model in all computations were more than 0.99, which shows a strong correlation.

As illustrated in Fig. 21, the c-parameter of the grouts containing MM and LPP remains similar to that of the reference at all dosages used in this study, while both HPP and diutan gum change this parameter dramatically. Diutan gum increases the c-parameter, which indicates that the true dynamic yield stress of the diutan gum grouts is higher than what presented by the Bingham model. On the other hand, HPP reduces the c-parameter and

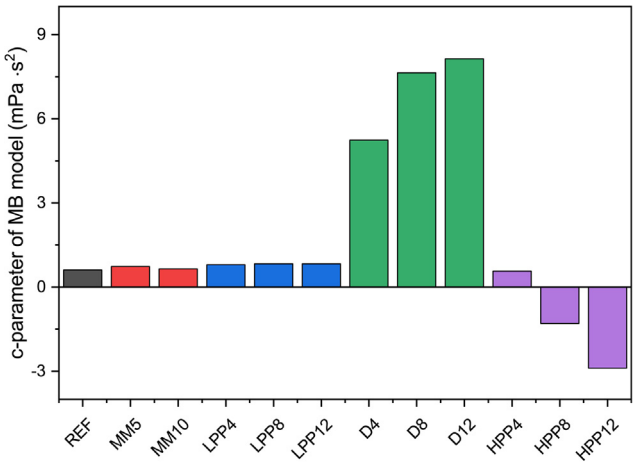

Fig. 20. c-parameter of the Modified Bingham model.

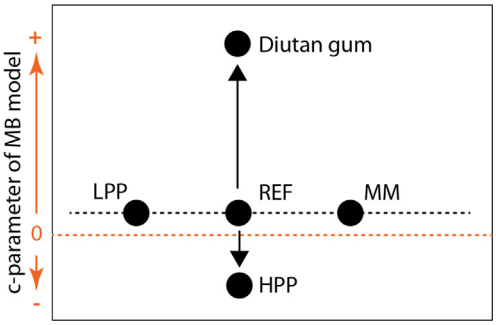

Fig. 21. c-parameter change by adding different VMAs.

changes its sign, which indicates that the true dynamic yield stress of the HPP grouts is lower than what is obtained from the Bingham model. The higher the dosage, the higher the effect.

In order to assess the influence of LPP and HPP on the fluidity of mortars, flow spread tests by mini-slump cone, at five different dosages, were performed. The ratio of water:cement:sand in the mortars was kept constant at 1:2:6, similar to EN 196–1 [67]. The flow spread tests were used to calculate the relative slump flow parameter (Γ) as follows

$$\Gamma = [d_1 + d_2/20]^2 - 1 \quad (4)$$

with Γ the relative slump flow, and d_1 and d_2 measured slump flows (cm). Some researchers [68] proposed to use this parameter to determine the minimum water demand to initiate flow (MWD) and relative water demand to increase fluidity (RWD) in mortars. With the objective to calculate MWD and RWD, a linear regression analysis between Γ and w/c is performed, where the intercept of the linear fit represents the MWD, and the slope of the linear fit represents the RWD [69].

This study proposes to use the relative slump flow to compare and contrast the influence of LPP with that of HPP on the fluidity of mortars by introducing two parameters: (1) minimum VMA demand to stop flow (MVD), and (2) relative VMA demand to decrease fluidity (RVD). With the objective to calculate MVD and RVD, a graph of the dosage of paper pulp axis and the relative slump axis is made. Then, a linear regression analysis is performed, in which the intercept of the linear regression equation represents minimum VMA demand to stop flow (MVD), and the absolute slope of the linear regression equation represents relative VMA demand to decrease fluidity (RVD). Fig. 22 displays these parameters along with the flow characteristics of the standard mortars having LPP and HPP. Incorporating HPP in mortars lowers the value of MVD by 35% and reduces the value of RVD by 31% in comparison to LPP. In other words, HPP more efficiently controls the fluidity of mortars by increasing viscosity.

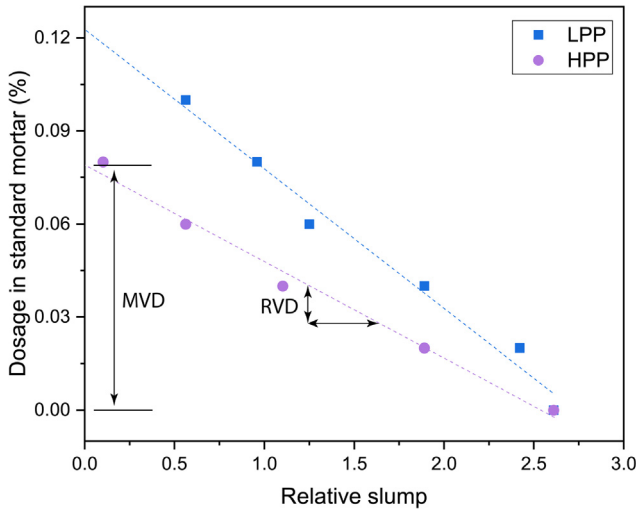

Fig. 22. Flow characteristics of the standard mortars having LPP and HPP, using the relative slump parameter, calculated based on the mini-slump flow test.

The small dosages of HPP and LPP needed for viscosity-modifying effect, have an insignificant effect on the hydration kinetics of cement grouts and flexural strength of mortars. However, they affect the compressive strength of mortars. Because of the differences in the variances of the compressive strength of mortars, Welch's ANOVA is used. Games-Howell grouping trend of compressive strengths of mortars at 95% confidence at different ages are shown in Fig. 23. VMAs that are not in an enclosed area are significantly different. The mean strength of HPP and LPP mortars are significantly different from that of the reference at one and seven days. The difference between LPP and the reference fades after 28 days as the grouping becomes broader and less variant. However, ultrafine milled paper pulp (HPP) continues to have significantly different compressive strength at 28 days.

The higher strength at early-age in mixtures containing HPP and LPP is in line with the findings on the compressive strength development in cement composites containing low dosages of cellulose filaments [70] and can stem from the bridging effect thanks to the developed bond between paper pulp filaments and cement hydration products. On the other hand, the lower early-age strength in mixtures containing diutan gum is in line with the findings on the low compressive strength of mixtures containing diutan gum [53] as a result of the low charge density of diutan gum and its tendency to adsorb out of mixing water and onto cement hydration products [54]. However, at later ages, as more hydration products are developed in mixtures, the influence of these characteristics in paper pulp and diutan gum diminishes, and the obvious difference in compressive strength after one day fades away after twenty-eight days.

In light of the fact that the main aim of this investigation is shedding more light on the versatility and the value that the milling process adds to paper pulp as a viscosity modifying admixture, various characteristics of cement composites containing HPP and LPP are tested in the first month after casting. Further research may investigate the durability of paper pulp in cement composites.

5. Conclusions

In the present research, the effects of fineness of milled paper pulp (LPP and HPP), obtained from different industrial mechanical milling levels of the same source of paper pulp, on the fresh and hardened properties of cement grouts are investigated. Two com-

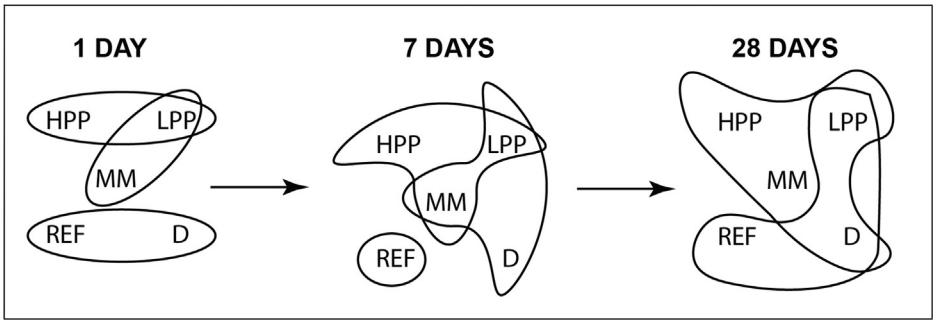

Fig. 23. Games-Howell grouping trend of compressive strengths of mortars at 95% confidence at different ages. VMAs that are not in an enclosed area are significantly different.

mercially available viscosity modifying admixtures, namely diutan gum and MasterMatrix, are used for comparison analysis. Based on the properties assessed and the results obtained, the following conclusions can be drawn:

- Milled paper pulp, made by mechanical milling, modifies the rheology of cement grouts and can be categorized as a sustainable VMA. The viscosity-modifying mechanism of paper pulp in cement grouts is a combination of bridging flocculation and swelling.
- High-energy milled paper pulp (HPP) consists mostly of the ultrafine fibers of the hierarchical structure of paper pulp and enhances both the plastic Bingham viscosity and dynamic yield stress of cement grouts more significantly than low-energy milled paper pulp (LPP).
- The range of the rheological effect of HPP on cement grouts is analogous to that of diutan gum at similar dosages. However, the ratio of the plastic viscosity to the yield stress in HPP is more significant than that of diutan gum grouts.
- The influence of the low-energy milled paper pulp (LPP) on the rheological behavior of cement grouts differs from that of the high-molecular-weight synthetic copolymer (MM) in that while the LPP mainly increases the plastic viscosity, the synthetic copolymer primarily changes the yield stress.
- The c-parameter of a second-order modified Bingham model is proposed to take the differences in the nonlinearity of grouts into account. While LPP and the high-molecular-weight synthetic copolymer (MM) do not influence the c-parameter of the cement grout, both HPP and diutan affect it significantly. Contrary to diutan gum that increases the c-parameter, HPP decreases it and makes its value negative. This change in sign of the c-parameter is an indicator that the true dynamic yield stress of the HPP grouts is lower than what is obtained from the Bingham model.
- Both LPP and HPP do not affect the hydration kinetics and thermal indicator of setting time. Besides, they both show good stability in a high alkaline environment.
- Welch's ANOVA confirms a significant difference in the average compressive strength of mortars with paper pulp with that of the reference. Games-Howel post hoc test shows that both LPP and HPP increase the 1-day and 7-day compressive strength of the mortars, compared to the reference. After 28 days, the significance of the difference between the compressive strength of reference mortars with that of LPP mortars fades but HPP mixtures continue to have higher compressive strength. A similar analysis shows that milled paper pulp does not affect the flexural strength of mortars at the dosages used for flow adjustment.

CRediT authorship contribution statement

H. Karimi: Conceptualization, Methodology, Investigation, Data curation, Formal analysis, Validation, Writing - original draft. **F. Gauvin:** Investigation, Writing - review & editing. **H.J.H. Brouwers:** Supervision, Funding acquisition, Writing - review & editing. **R. Cardinaels:** Writing - review & editing. **Qingliang Yu:** Conceptualization, Supervision, Funding acquisition, Project administration, Writing - review & editing.

Declaration of Competing Interest

The authors declare that they have no known competing financial interests or personal relationships that could have appeared to influence the work reported in this paper.

Acknowledgments

This research is in cooperation with Sappi Nederland Services BV. Dr. L. Xu and Dr. M. Jennekens are thanked for initiating the collaboration, and Ir. R. Claessen, Dr. L. Tufano and Dr. L. Xu are thanked for the fruitful discussions throughout the project.

References

[1] A. Blanco, C. Negro, C. Monte, E. Fuente, J. Tijero, Peer Reviewed: The Challenges of Sustainable Papermaking, Environ. Sci. Technol. 38 (2004) 414A–420A, https://doi.org/10.1021/es040654y.
[2] P. Berg O. Lingqvist Pulp, Paper, and packaging in the next decade: Transformational change, McKinsey Co., Pap. For Prod. 2017 1 18
[3] P. Bajpai, Uses of Recovered Paper Other than Papermaking, Recycl, Deinking Recover. Pap. (2014) 283–295, https://doi.org/10.1016/B978-0-12-416998-2.00016-7.
[4] D. Gavrilescu, Energy from biomass in pulp and paper mills, Environ. Eng. Manag. J. 7 (2008) 537–546.
[5] Statista, Cement Industry in the US (report) 47 2018 www.statista.com
[6] WBCSD, The Cement Sustainability Initiative, Recycling Concrete, WBCSD, 2009. www.wbcsdcement.org.
[7] Global Market Insights, Concrete Admixture Market Share - Industry Size Forecast Report 2024, 2018. www.gminsights.com.
[8] C. Correia, S. Francisco, R. Soares, H. Savastano, Nanofibrillated cellulose and cellulosic pulp for reinforcement of the extruded cement based materials, Constr. Build. Mater. 160 (2018) 376–384, https://doi.org/10.1016/j.conbuildmat.2017.11.066.
[9] E.F. Campello, M.V. Pereira, F.A. Darwish, K. Ghavami, On the Fatigue Behavior of Bamboo Pulp Reinforced Cementitious Composites, Procedia Struct. Integr. 2 (2016) 2929–2935, https://doi.org/10.1016/j.prostr.2016.06.366.
[10] C. De Souza Rodrigues, K. Ghavami, P. Stroeven, Porosity and water permeability of rice husk ash-blended cement composites reinforced with bamboo pulp, in, J. Mater. Sci., Kluwer Academic Publishers-Plenum Publishers (2006) 6925–6937, https://doi.org/10.1007/s10853-006-0217-2.
[11] R.S.P. Coutts, Y. Ni, B.C. Tobias, Air-cured bamboo pulp reinforced cement, J. Mater. Sci. Lett. 13 (1994) 283–285, https://doi.org/10.1007/BF00571777.
[12] M. Khorami, E. Ganjian, A. Srivastav, Feasibility Study on Production of Fiber Cement Board Using Waste Kraft Pulp in Corporation with Polypropylene and Acrylic Fibers, Mater. Today Proc. 3 (2016) 376–380, https://doi.org/10.1016/J.MATPR.2016.01.023.
[13] G.H.D. Tonoli, R.F. Mendes, G. Siqueira, J. Bras, M.N. Belgacem, H. Savastano, Isocyanate-treated cellulose pulp and its effect on the alkali resistance and performance of fiber cement composites, Holzforschung. 67 (2013) 853–861, https://doi.org/10.1515/hf-2012-0195.
[14] M. Khorami, E. Ganjian, The effect of limestone powder, silica fume and fibre content on flexural behaviour of cement composite reinforced by waste Kraft pulp, Constr. Build. Mater. 46 (2013) 142–149, https://doi.org/10.1016/j.conbuildmat.2013.03.099.
[15] B.J. Mohr, J.J. Biernacki, K.E. Kurtis, Supplementary cementitious materials for mitigating degradation of kraft pulp fiber-cement composites, Cem. Concr. Res. 37 (2007) 1531–1543, https://doi.org/10.1016/j.cemconres.2007.08.001.
[16] N.H. El-Ashkar, H. Nanko, K.E. Kurtis, Effect of Moisture State on Mechanical Behavior and Microstructure of Pulp Fiber-Cement Mortars, J. Mater. Civ. Eng. 19 (2007) 691–699, https://doi.org/10.1061/(ASCE)0899-1561(2007)19:8(691).
[17] B.J. Mohr, J.J. Biernacki, K.E. Kurtis, Microstructural and chemical effects of wet/dry cycling on pulp fiber–cement composites, Cem. Concr. Res. 36 (2006) 1240–1251, https://doi.org/10.1016/J.CEMCONRES.2006.03.020.
[18] M.M. Shokrieh, A. Mahmoudi, H.R. Shadkam, Hybrid polyvinyl alcohol and cellulose fiber pulp instead of asbestos fibers in cement-based composites, Mech. Compos. Mater. 51 (2015) 231–238, https://doi.org/10.1007/s11029-015-9494-7.
[19] J. Claramunt, M. Ardanuy, L.J. Fernandez-Carrasco, Wet/Dry Cycling Durability of Cement Mortar Composites Reinforced with Micro- and Nanoscale Cellulose Pulps, BioResources. 10 (2015) 2681–2685, https://doi.org/10.1021/bi00834a066.
[20] J.E.M. Ballesteros, S.F. Santos, G. Mármol, H. Savastano, J. Fiorelli, Evaluation of cellulosic pulps treated by hornification as reinforcement of cementitious composites, Constr. Build. Mater. 100 (2015) 83–90, https://doi.org/10.1016/j.conbuildmat.2015.09.044.
[21] G.H. Denzin Tonoli, A.E.F. De Souza Almeida, M.A. Pereira-Da-Silva, A. Bassa, D. Oyakawa, H. Savastano, Surface properties of eucalyptus pulp fibres as reinforcement of cement-based composites, Holzforschung. 64 (2010) 595–601, https://doi.org/10.1515/HF.2010.073.
[22] G.H.D. Tonoli, H. Savastano, E. Fuente, C. Negro, A. Blanco, F.A. Rocco Lahr, Eucalyptus pulp fibres as alternative reinforcement to engineered cement-based composites, Ind. Crops Prod. 31 (2010) 225–232, https://doi.org/10.1016/J.INDCROP.2009.10.009.
[23] G. Mármol, S.F. Santos, H. Savastano, M.V. Borrachero, J. Monzó, J. Payá, Mechanical and physical performance of low alkalinity cementitious composites reinforced with recycled cellulosic fibres pulp from cement kraft

bags, Ind. Crops Prod. 49 (2013) 422–427, https://doi.org/10.1016/J.INDCROP.2013.04.051.
[24] G.H.D. Tonoli, A.P. Joaquim, M.A. Arsne, K. Bilba, H. Savastano, Performance and durability of cement based composites reinforced with refined sisal pulp, Mater. Manuf. Process. 22 (2007) 149–156, https://doi.org/10.1080/10426910601062065.
[25] H. Savastano, P.G. Warden, R.S.P. Coutts, Mechanically pulped sisal as reinforcement in cementitious matrices, Cem. Concr. Compos. 25 (2003) 311–319, https://doi.org/10.1016/S0958-9465(02)00055-0.
[26] R. Hosseinpourpia, P. Hosseini, S.R. Mofidian, R. Hosseinpourpia, A. Varshoee, Influence of Nanosilica on Properties of Green Cementitious Composites Filled with Waste Sulfite Pulp Fiber and Aminosilane, Arab. J. Sci. Eng. 39 (2014) 2631–2640, https://doi.org/10.1007/s13369-013-0935-0.
[27] P. Jongvisuttisun, C. Negrello, K.E. Kurtis, Effect of processing variables on efficiency of eucalyptus pulps for internal curing, Cem. Concr. Compos. 37 (2013) 126–135, https://doi.org/10.1016/j.cemconcomp.2012.11.006.
[28] A. Mezencevova, V. Garas, H. Nanko, K.E. Kurtis, Influence of Thermomechanical Pulp Fiber Compositions on Internal Curing of Cementitious Materials, J. Mater. Civ. Eng. 24 (2012) 970–975, https://doi.org/10.1061/(ASCE)MT.1943-5533.0000446.
[29] R.K. Johnson, A. Zink-Sharp, S.H. Renneckar, W.G. Glasser, A new bio-based nanocomposite: Fibrillated TEMPO-oxidized celluloses in hydroxypropylcellulose matrix, Cellulose. 16 (2009) 227–238, https://doi.org/10.1007/s10570-008-9269-6.
[30] K.H. Khayat, N. Mikanovic, Viscosity-enhancing admixtures and the rheology of concrete, in: Underst. Rheol. Concr., 2011: pp. 209–228. https://doi.org/10.1016/B978-0-85709-028-7.50008-X.
[31] American Concrete Institute, Farmington Hills (2007).
[32] K.H. Khayat, Effects of antiwashout admixtures on properties of hardened concrete, ACI Mater. J. 93 (1996) 134–146. https://doi.org/10.14359/1412.
[33] W. Li, Z. Huang, F. Cao, Z. Sun, S.P. Shah, Effects of nano-silica and nano-limestone on flowability and mechanical properties of ultra-high-performance concrete matrix, Constr. Build. Mater. 95 (2015) 366–374, https://doi.org/10.1016/j.conbuildmat.2015.05.137.
[34] W. Li, Z. Huang, T. Zu, C. Shi, W.H. Duan, S.P. Shah, Influence of nanolimestone on the hydration, mechanical strength, and autogenous shrinkage of ultrahigh-performance concrete, J. Mater. Civ. Eng. 28 (2016) 04015068, https://doi.org/10.1061/(ASCE)MT.1943-5533.0001327.
[35] W. Li, Z. Huang, G. Hu, W. Hui Duan, S.P. Shah, Early-age shrinkage development of ultra-high-performance concrete under heat curing treatment, Constr. Build. Mater. 131 (2017) 767–774, https://doi.org/10.1016/j.conbuildmat.2016.11.024.
[36] J. Ouyang, B. Han, Y. Cao, W. Zhou, W. Li, S.P. Shah, The role and interaction of superplasticizer and emulsifier in fresh cement asphalt emulsion paste through rheology study, Constr. Build. Mater. 125 (2016) 643–653, https://doi.org/10.1016/j.conbuildmat.2016.08.085.
[37] A. Leemann, F. Winnefeld, The effect of viscosity modifying agents on mortar and concrete, Cem. Concr. Compos. 29 (2007) 341–349, https://doi.org/10.1016/j.cemconcomp.2007.01.004.
[38] O.M. Jensen, Use of superabsorbent polymers in construction materials, in: 1st Int. Conf. Microstruct. Relat. Durab. Cem. Compos. 13-15 Oct., Nanjing, China, 2008: pp. 757–764.
[39] X. Sun, Q. Wu, J. Zhang, Y. Qing, Y. Wu, S. Lee, Rheology, curing temperature and mechanical performance of oil well cement: Combined effect of cellulose nanofibers and graphene nano-platelets, Mater. Des. 114 (2017) 92–101, https://doi.org/10.1016/j.matdes.2016.10.050.
[40] M. Chen, L. Li, Y. Zheng, P. Zhao, L. Lu, X. Cheng, Rheological and mechanical properties of admixtures modified 3D printing sulphoaluminate cementitious materials, Constr. Build. Mater. 189 (2018) 601–611, https://doi.org/10.1016/j.conbuildmat.2018.09.037.
[41] International Organization for Standardization (2014).
[42] ENCI, Portland Cement, CEM I 52,5 R, Technical Advice, 's-Hertogenbosch, 2017. www.enci.nl.
[43] D. Han, R.D. Ferron, Influence of high mixing intensity on rheology, hydration, and microstructure of fresh state cement paste, Cem. Concr. Res. 84 (2016) 95–106, https://doi.org/10.1016/j.cemconres.2016.03.004.
[44] H. Karimi, Q.L. Yu, H.J.H. Brouwers, Evaluation of a novel cellulose-based viscosity modifying admixture in rheological properties of cementitious pastes, in: V. Bílek, H. Šimonová, Z. Keršner (Eds.), 6th Int. Conf. Non-Traditional Cem. Concr. June 19–22, NOVPRESS, Brno, 2017: pp. 172–179.
[45] X. Sun, Q. Wu, S. Lee, Y. Qing, Y. Wu, Cellulose Nanofibers as a Modifier for Rheology, Curing and Mechanical Performance of Oil Well Cement, Sci. Rep. 6 (2016) 31654, https://doi.org/10.1038/srep31654.
[46] A. Yahia, K.H. Khayat, Applicability of rheological models to high-performance grouts containing supplementary cementitious materials and viscosity enhancing admixture, Mater. Struct. 36 (2003) 402–412, https://doi.org/10.1007/BF02481066.
[47] West Conshohocken (2014), https://doi.org/10.1520/C1679-14.
[48] West Conshohocken (2014), https://doi.org/10.1520/C1698-09R14.
[49] ASTM, ASTM C191 - 13 Standard Test Methods for Time of Setting of Hydraulic Cement by Vicat Needle, (n.d.). https://www.astm.org/Standards/C191.htm (accessed January 16, 2018).
[50] P. Coussot, Introduction to the rheology of complex fluids, in: Underst. Rheol. Concr., Woodhead Publishing, 2011: pp. 3–22. https://doi.org/10.1016/B978-0-85709-028-7.50001-7.
[51] K. Bilba, M.A. Arsene, A. Ouensanga, Sugar cane bagasse fibre reinforced cement composites. Part I. Influence of the botanical components of bagasse on the setting of bagasse/cement composite, Cem. Concr. Compos. 25 (2003) 91–96, https://doi.org/10.1016/S0958-9465(02)00003-3.
[52] O. Onuaguluchi, N. Banthia, Plant-based natural fibre reinforced cement composites: A review, Cem. Concr. Compos. 68 (2016) 96–108, https://doi.org/10.1016/j.cemconcomp.2016.02.014.
[53] C. Ciobanu, • I Lazău Lazău, • C Păcurariu Păcurariu, Investigation regarding the effect of viscosity modifying admixtures upon the Portland cement hydration using thermal analysis, (n.d.). https://doi.org/10.1007/s10973-012-2655-1.
[54] M. Sonebi, Rheological properties of grouts with viscosity modifying agents as diutan gum and welan gum incorporating pulverised fly ash, Cem. Concr. Res. 36 (2006) 1609–1618, https://doi.org/10.1016/j.cemconres.2006.05.016.
[55] B. Abderrahim, E. Abderrahman, A. Mohamed, T. Fatima, T. Abdesselam, O. Krim, Kinetic Thermal Degradation of Cellulose, Polybutylene Succinate and a Green Composite: Comparative Study, World J. Environ. Eng. Vol. 3, 2015, Pages 95-110. 3 (2015) 95–110. https://doi.org/10.12691/WJEE-3-4-1.
[56] M. Palacios, R.J. Flatt, Working mechanism of viscosity-modifying admixtures, in: Sci. Technol. Concr. Admixtures, 2015: pp. 415–432. https://doi.org/10.1016/B978-0-08-100693-1.00020-5.
[57] W. Schmidt, H.J.H. Brouwers, H.-C. Kühne, B. Meng, The Working Mechanism of Starch and Diutan Gum in Cementitious and Limestone Dispersions in Presence of Polycarboxylate Ether Superplasticizers, Appl. Rheol. 23 (2013), https://doi.org/10.3933/ApplRheol-23-52903.
[58] M.A. Bury, B.J. Christensen, Role of innovative chemical admixtures in producing self-consolidating concrete, First North Am, Conf. Des. Use Self-Consol. Concr. (2002) 137–141.
[59] K. Yoshioka, E.I. Tazawa, K. Kawai, T. Enohata, Adsorption characteristics of superplasticizers on cement component minerals, Cem. Concr. Res. 32 (2002) 1507–1513, https://doi.org/10.1016/S0008-8846(02)00782-2.
[60] M. Cyr, M. Mouret, Rheological Characterization of Superplasticized Cement Pastes Containing Mineral Admixtures: Consequences on Self-Compacting Concrete Design, in: Proc. Seventh CANMET/ACI Int. Conf. Superplast. Other Chem. Admixtures Concr., 2003: pp. 241–256. https://www.concrete.org/publications/internationalconcreteabstractsportal/m/details/id/12917.
[61] C.Z. Li, N.Q. Feng, Y. De Li, R.J. Chen, Effects of polyethlene oxide chains on the performance of polycarboxylate-type water-reducers, Cem. Concr. Res. 35 (2005) 867–873, https://doi.org/10.1016/j.cemconres.2004.04.031.
[62] S. Hanehara, K. Yamada, Interaction between cement and chemical admixture from the point of cement hydration, absorption behaviour of admixture, and paste rheology, Cem. Concr. Res. 29 (1999) 1159–1165, https://doi.org/10.1016/S0008-8846(99)00004-6.
[63] O. Blask, D. Honert, The Electrostatic Potential of Highly Filled Cement Suspension Containing Various Superplasticizers, in: Seventh CANMET/ACI Int. Symp. Superplast. Other Chem. Admixtures Concr. Malhotra, V.M, 2003: pp. 87–101. https://doi.org/10.14359/12907.
[64] A. Yahia, S. Mantellato, R.J. Flatt, Concrete rheology, in: Sci. Technol. Concr. Admixtures, Elsevier, 2016: pp. 97–127. https://doi.org/10.1016/B978-0-08-100693-1.00007-2.
[65] A. Yahia, K. Khayat, Analytical models for estimating yield stress of high-performance pseudoplastic grout, Cem. Concr. Res. 31 (2001) 731–738, https://doi.org/10.1016/S0008-8846(01)00476-8.
[66] K.H. Khayat, A. Yahia, Effect of Welan Gum-High-Range Water Reducer Combinations on Rheology of Cement Grout, ACI Mater. J. 94 (1997) 365–372. https://doi.org/10.14359/321.
[67] Determination of strength, BSI (2016).
[68] H. Okamura M. Ouchi Self-Compacting, Concrete 2003
[69] I. Mehdipour, Characterization and performance of eco and crack-free high-performance concrete for sustainable infrastructure (Doctoral dissertation), Missouri University of Science and Technology, 2017.
[70] O.A. Hisseine, N. Basic, A.F. Omran, A. Tagnit-Hamou, Feasibility of using cellulose filaments as a viscosity modifying agent in self-consolidating concrete, Cem. Concr. Compos. 94 (2018) 327–340, https://doi.org/10.1016/j.cemconcomp.2018.09.009.